Original Article

Influence of injection molding parameters on the morphology, mechanical and surface properties of ABS foams

J. GÓMEZ-MONTERDE

SEAT SA. Autovía A-2, km 585. Apartado de correos 91, E-08760 Martorell, Spain.

M. SÁNCHEZ-SOTO, M. LL. MASPOCH

Centre Català del Plàstic, Universitat Politècnica de Catalunya-BarcelonaTech (ETSEIB, ETSEIAT). Carrer Colom 114, E-08222 Terrassa, Spain.

*Corresponding author:

Javier Gómez-Monterde (E-mail: javier.gomez@upc.edu / Telephone: +34 93 7731113)

ABSTRACT

In this work, microcellular ABS foams were studied. A series of injection molding samples defined by a design of experiments were carried out to analyze the effect of shot volume, mold temperature and injection velocity on the morphology, mechanical properties and surface roughness of microcellular samples. A predominant influence of shot volume on the cell structure and tensile properties was evidenced. Higher cell densities and narrower cell size distributions were obtained at lower injection volume. However, elastic modulus and tensile strength were improved by increasing the shot size. The effect of mold temperature and injection velocity was secondary. Higher levels of mold temperature and injection rate provided finer cell morphologies, but their effects on the elastic modulus and tensile strength were negligible. The decrease in shot volume and increase in gas content led to poor surface quality, whereas it was greatly improved by raising both mold temperature and injection velocity.

KEYWORDS

Foams, injection molding, mechanical properties, morphology, surfaces.

INTRODUCTION

Lightweight design is one of the most important challenges in automotive industry, due to regulatory constraints and the aim of reducing weight, energy consumption and greenhouse gas emissions. Among the different strategies conducted to achieve lighter automobiles, car

manufacturers focus their efforts on replacing metals with polymers and increasing the specific strengths and rigidities of polymers.[1]

Injection molding is one of the most common methods for large-scale production of thermoplastic parts. Thus, foaming by injection molding techniques, such as the microcellular injection molding *MuCell®* process (*Trexel Inc.*), arises as a great chance to reduce weight in plastic components. Indeed, Elduque *et al.*[2] as well as Kim and Wallington[3] found that by microcellular injection molding, it is possible not only to lighten industrial components, but also to decrease carbon footprint and emissions. The *MuCell®* technology is a physical foaming method consisting of four main steps: gas dissolution, cell nucleation, cell growth and shaping in the mold. First, the gas is dissolved at supercritical pressure and temperature in the molten polymer in the barrel of the injection molding machine. When the gas/polymer single-phase solution fills the mold, the pressure drop induces a thermodynamic instability promoting the nucleation of millions of cells. These cells grow and expand by diffusion of the gas into already existing bubbles, until the polymer solidifies shaping the final part. As a result, lighter, cheaper and more environmentally friendly components are produced, with improved dimensional stability and reduced cycle time.

The final quality of the conventional injection molded parts is influenced by several factors, such as the material, the model design and process conditions. The introduction of gas in microcellular injection molding increases the number of variables controlling the manufacturing process. Many investigations have been carried out on the relationship between processing parameters, cell structure and mechanical properties of different foamed materials, including thermoplastic blends[4] and polymer composites.[5] Xu[6] provided

an extensive description of the effect of the processing parameters on the foam morphology and properties, concluding that injection velocity, gas dosing and content, mold temperature and shot volume are the most influencing ones. Empirical models for an accurate control of the supercritical fluid dosage have been developed, in order to ensure high part quality and consistency.[7] However, establishing direct relationships between processing parameters and cell structure and mechanical characteristics is not always satisfactory and sometimes even contradictory, because of dependence on polymer material properties and part geometry. Additionally, surface defects such as swirl marks, silver streaks and large surface roughness are usually found in microcellular parts foamed with physical blowing agents, and different solutions based on mold technologies have been introduced to improve the surface quality, like Gas Counter Pressure, Rapid Heating Cycle Molding, Film Insulation or Co-injection Molding.[8,9]

In this study, microcellular rigid foam components of ABS were produced. This material is a multiphase polymer consisting of acrylonitrile, which contributes to a better chemical resistance and dimensional stability, butadiene, enhancing ductility, and styrene, providing stiffness and easing processing, with a wide range of applications. Most of researches performed on ABS foams so far have been conducted in batch processes.[10,11] Lin *et al.*[12] reported a great capability of gas absorption of ABS due to its amorphous nature. In reference to foaming by injection molding, recently Dong *et al.*[13] employed ABS foams to describe the governing cell forming mechanisms during filling and post-filling stages. However, few studies have focused on the influence of the injection molding parameters on the cell structure and properties of this material.[14]

The aim of this work is to analyze the effect of different processing parameters, particularly shot volume, mold temperature and injection velocity, on the morphology, mechanical properties and surface roughness of ABS foams obtained by microcellular injection molding.

MATERIALS AND METHODS

Material

A commercial grade of ABS (*Magnum™ 8434*) widely used for automotive interior trims was employed in the present study. It has a density of 1.05 g cm^{-3} (ISO 1183/B) and a melt flow index of 13 g 10 min^{-1} (ISO 1133), and it was supplied by *Styron Netherlands B.V.*

Injection molding

Cylindrical bars of 300 mm in length and diameters of 4, 5 and 8 mm (Figure 1) were injection molded in a *Victory 110* injection molding machine (*Engel GmbH*), with a clamping force of 1100 kN, a diameter of the screw of 40 mm and equipped with *MuCell®* supercritical fluid (SCF) supply system. Nitrogen (N_2) was employed as physical blowing agent.

The material was previously dried at 80 ºC for a minimum of 4 hours in a *DSN560HE* dehumidifier (*PIOVAN*) with a dew point of -40 ºC, so as to avoid moisture problems during processing. In order to study the effect of shot volume, mold temperature and injection velocity on the morphology, mechanical properties and surface roughness of foamed bars, a design of experiments with three variables and two levels were defined (Table 1).

As a full 2^3 factorial design, 8 different injection molding conditions (C1-C8) outlined in Table 2 were used to fabricate the bars. One additional series, labeled C0, was conducted at

medium levels of experimental settings, in order to check linearity of the effects of the different factors. Preliminary experiments were carried out to determine the variation range of injection molding and foaming parameters. It was concluded that the minimum shot volume to ensure a complete filling of the mold cavities when foaming was 68 cm^3, which corresponds to a 17% of weight reduction as compared to the unfoamed counterpart. Then, a lower foaming ratio was set (10% of weight reduction) in order to adequately study the morphology and tensile properties variations. Thus, both levels (-1 and 1) of the shot volume were adjusted to achieve a 17% and a 10% of weight reduction, respectively. The content of the blowing agent (N$_2$) was 0.93% for the former series of foamed bars (17% of weight reduction) and 0.60% for the latter (10% of weight reduction), and was kept at 0.80% for the intermediate series C0. After the injection procedure, the bars were weighed and their volume was measured to calculate the real weight reduction ratio obtained by the different processing conditions.

In all experiments both the melt temperature profile and cooling time were kept constant. The melt temperature from hopper to nozzle was 160-220-230-245-250 ºC. On the other hand, the cooling time was set to 30 seconds, due to the large thickness of the bars (Ø = 8 mm). Solid samples were injection molded with a shot volume of 85 cm^3, an injection velocity of 70 cm^3 s^{-1} and a mold temperature of 60 ºC. The holding pressure was 60 MPa and was applied for 10 seconds. Injection time for solid bars and C0 series (injected at 70 cm^3 s^{-1} velocity) was 1.6 s, whereas it was around 2.2 s for the foamed series with the lowest injection velocity (C1, C3, C5 and C7, injected at 40 cm^3 s^{-1}), and 1.1 s for the foamed conditions obtained with the highest velocity (C2, C4, C6 and C8, injected at 100 cm^3 s^{-1}).

Characterization

Morphology

The morphology of the foamed specimens was analyzed at the 5 mm cross-section of bar A, as shown in Figure 1. Samples were submitted to cryogenic fracture, and the resulting fracture surfaces were examined by *Scanning Electron Microscopy* (SEM) using a *JEOL JSM-560* microscope. Micrographs were adjusted for an appropriate level of contrast and morphological parameters, such as cell size, cell density and skin thickness were determined with the aid of *Igor Pro®* (*Wavemetrics Inc.*) and *Matlab®* (*The MathWorks Inc.*) software. Cell density (*N*) represents the number of cells per volume (cells cm^{-3}) and it is calculated as follows[15]:

$$N = \left(\frac{n}{A}\right)^{\frac{3}{2}} \left(\frac{\rho_s}{\rho_f}\right),\tag{1}$$

where *n* is the number of cells in the micrograph, *A* is the analyzed area (cm^2) and ρ_s and ρ_f are the density of solid and foamed material, respectively. The area of each cell of the micrograph was measured and, assuming all of them were completely spherical, an equivalent cell diameter or cell size (*d*) was determined.

The *Cell Distribution Index* (*CDI*) was proposed by Rizvi *et al.*[16] to assess the uniformity of cell size distribution, and it is defined as:

$$CDI = \frac{\overline{d_w}}{\overline{d_n}}.\tag{2}$$

Here, $\overline{d_w}$ and $\overline{d_n}$ are the diameter average cell diameter and number average cell diameter, respectively, calculated by means of the number of cells (n_i) with the same equivalent diameter (d_i):

$$\overline{d_w} = \frac{\sum_i n_i d_i^2}{\sum_i n_i d_i} \tag{3}$$

$$\overline{d_n} = \frac{\sum_i n_i d_i}{\sum_i n_i} \tag{4}$$

Mechanical properties

Mechanical properties were assessed through tensile tests made on samples of 5 mm in diameter and a length of 110 mm extracted from the injected bars (Figure 1). A minimum of 5 specimens of each condition were tested in a universal testing machine *Zwick/Roell Amsler HC25/2008* (*Zwick GmbH & Co. KG*), at a crosshead speed of 50 mm min^{-1} under room temperature, following the recommendations given by the ISO 527 standard. The initial distance between clamps was 50 mm.

Surface roughness

The topography of the solid and foamed samples was assessed on the top surfaces of the bars (Figure 1) by means of a non-contact, white light interferometer (*FRT MicroProf 200, Fries Research & Technology*). An area of 3x3 mm^2 from each specimen was measured with a sensor of 3000 µm, using a sampling length of 0.003 mm and a cut-off of 0.429 mm. The surface roughness was determined through two parameters: the Average roughness (S_a) and the Root mean square (S_q), calculated as indicated in ISO 25178-2: 2012 standard:

$$S_a = \frac{1}{A} \int \int_A z(x,y) \, dxdy \tag{5}$$

$$S_q = \sqrt{\frac{1}{A} \int \int_A z^2(x,y) \, dxdy} \tag{6}$$

where $z(x, y)$ denotes the surface height measured at the coordinates (x, y) within the area A.

RESULTS AND DISCUSSION

Morphology

The SEM micrographs corresponding to the cross-sections of the different injected bars are shown in Figures 2 and 3. The material structure of the foamed samples consists of a solid external layer and a foamed core. As a consequence of the temperature gradient from the surface to the middle of the part, different cell morphologies are developed and therefore this foamed core can be divided into two different areas (Figure 4). The high heat concentration and slow cooling in the center of the bars makes the polymer viscosity in the region to be insufficient to prevent massive cell coalescence and expansion in the nucleus area, forming bigger bubbles heterogeneously dispersed. Between the nucleus and the solid skin, there is a transition region with cells smaller than 100 µm uniformly distributed (microcellular area). A similar structure was reported by Bledzki *et al.*[17] with microcellular Polycarbonate.

Regarding the shape of the cells shown in Figure 2(a) and Figure 3(a), near the surface layer cells are distorted following the circumferential shape of the cross-section, but they become more spherical as they get closer to the center. Qualitatively, samples with 17% of weight reduction (Figure 3(a)) seem to present finer cell structures, with a higher number of smaller cells and more homogenous cell distribution than bars foamed with 10% of weight reduction (Figure 2(a)). These remarks are in agreement with the morphological parameters summarized in Table 3. The solid skin thickness varies from 0.25 to 0.36 mm. The cell density is kept in an order of magnitude of 10^6 cells cm^{-3} in all cases. This can be explained by the nucleating effect of rubber particles of ABS found by Tsuchiya *et al.*[18], as well as by the high diffusivity of N_2 in ABS reported by Hwang and Cha[19]. According to the study carried out by Sorrentino *et al.*[15] with PET foams, a high diffusivity of the gas in the polymer leads to an increase in cell density and a reduction in cell diameter. Figure 2(b) and Figure 3(b) depict the cell size distribution of samples with both levels of weight reduction. The minimum diameter which was possible to measure due to the resolution of the micrographs was 8 μm. Despite the wide range of cell size obtained, around 95% of cells were smaller than 50 μm, with a center value of 20 μm. The suitability for use this materials with smaller or bigger cells in automotive applications will be determined by their influence on the mechanical properties and the allowed limits in such applications.

The *Cell Distribution Index* (*CDI*) is a polydispersity index parameter evaluating the uniformity in cell size. Thus, a *CDI* value close to unity represents monodispersity and higher values indicate greater differences in cell sizes. According to the results provided in Table 3, the *CDI* varies from 1.50 to 2.00, due to the wide cell size range of the foams obtained

under the different injection conditions. Gómez-Monterde et al.[20] reported narrower cell size distributions (6-47 µm) and higher cell densities (10^7 cells cm^{-3}) of ABS foams injected into 5 mm-thick plates with similar levels of weight reduction. The influence of the part geometry on the cell structure is then evidenced comparing the morphological parameters of both foamed samples made of the same material.

Mechanical properties

The engineering stress-strain curves of solid and foamed samples (C4, C0 and C8) obtained from tensile tests are shown in Figure 5. Due to the similar curves found in the samples with the same levels of weight reduction (10% - C1, C2, C3 and C4 on one hand, and 17% - C5, C6, C7 and C8 on the other), only one representative curve of each level of weight reduction (C4 and C8) was represented in Figure 5 for a better interpretation of the effect of shot volume on the mechanical behavior of the parts (solid, 10% of weight reduction (C4), 13% of weight reduction (C0) and 17% of weight reduction (C8)).

The results of elastic modulus, stress and strain at yield point and ultimate strength of solid and foamed bars at different processing conditions are summarized in Figure 6. All specimens reached the yield point followed by necking and plastic deformation prior to breaking. As reported by Beydokhti et al.[21] working on ABS composites, foaming reduces gradually the elastic modulus and tensile strength as the density decreases. The specific modulus and tensile strength, defined as the ratio between these properties and the

apparent density, remain almost constant and at the same order of magnitude as the solid samples.

Yin and Wang[22] pointed out that crazing is the main plastic deformation mechanism of ABS. Foamed samples are more brittle than the solid counterparts due the presence of cells in the core, as can be observed in Figure 5 by comparing the elongation at break of the different solid and foamed series. The elongation at break was excluded from the studied effects because of the large scatter observed in this parameter. In any case, the stress-strain curves depicted in Figure 5 correspond to the average behavior of the samples tested in each plotted condition. Finally, it is worth to notice the same level of yield strain ($\varepsilon_y \approx 2.40$) and ultimate strength ($\sigma_u \approx 30$ MPa) obtained in all solid and foamed materials.

Surface roughness

Surface topographies of solid and foamed samples (C5) are illustrated in Figure 7. A smoother surface in solid bars can be clearly seen from both pictures. When foaming, the melt flow front pushes cells from the core to the surface cavity, where they are stretched and frozen, resulting in a surface with several defects.[23] These observations are in agreement with the increase in Average roughness (S_a) and the Root mean square (S_q) parameters of the foamed samples, as summarized in Figure 8.

Within foamed series, it can be seen that the surface roughness increases with the amount of injected gas. However, this trend is only evident at low mold temperature and injection

velocity, remarking a strong influence of these injection molding parameters on the surface quality of the parts. These effects will be discussed in the sections below.

Analysis of the factorial design

The experimental results obtained from the morphology, mechanical and surface characterizations were collected and underwent statistical analysis. Then, the influence of the processing parameters on the cell structure, mechanical properties and surface roughness was determined. As an example of analysis, Figure 9 shows the main effect of shot volume, mold temperature and injection velocity on the skin thickness. The results of intermediate condition C0 are plotted as individual points. As they do not fit the line joining the extreme values, it could seem that there is no perfect linearity between the factors and the response variables. However, it should be noted that the variations in the solid skin thickness range from 0.29 to 0.32 mm and therefore clear tendencies are difficult to be drawn. Moreover, the addition of central points does not affect the usual effects estimated in the factorial design.[24] The analysis of curvature and variance cannot be performed considering all factors included in the model. At least one degree of freedom is required, so the *Backward* method of regression stepwise technique[25] was employed to remove factors with the smallest contribution to the response. The significance level *α* for this procedure was taken as 0.05.

The simplified regression models for each morphological tensile and surface roughness parameter are summarized in Table 4. Following the example with skin thickness, the analysis of variance (ANOVA) is shown in Table 5. The *Sum of Squares*, *Mean Square*, *F-*

value and *p-value* were calculated according to the equations and guidelines given by Montgomery[24] All factors and interactions with a *p-value* lower than the confidence level (α = 0.05) are significant, that is, they have a remarkable effect on the response when moving from one level to another, and cannot be neglected in the regression models of Table 4. Through the ANOVA analysis, it can be seen that the curvature is not significant for skin thickness response, as has been already commented above due to the narrow range of variation. However, there is an interaction between parameters which needs to be considered. When interactions occur, the factors cannot be evaluated individually.[26] The presence of interaction between factors is discussed in the corresponding section below.

As a general trend, the shot volume was the most influencing factor on the studied morphology and tensile properties. On the contrary, the rest of injection molding parameters had a greater effect on the surface quality. Therefore for a better visualization of the effect of mold temperature and injection velocity on the response variables (weight reduction, solid skin thickness, cell density, maximum cell size, *CDI*, *E*, σ_y, S_a and S_q), they are displayed separately in Figures 9 and 10 for each level of shot volume.

Effect of shot volume

As expected, Figure 10 evinces that both cell structure and mechanical properties are more dependent on shot volume than upon mold temperature and injection rate. Since this parameter corresponds to the amount of material injected into the cavity mold, it determines the final weight and density of the part. Obviously, a higher shot volume results in lower weight reduction ratio, and vice versa.

In order to fill completely the mold cavity, the SCF content was increased as the level of shot volume decreased (0.93% for foamed bars with 17% of weight reduction; 0.60% for 10% of weight reduction, and 0.80% for the intermediate series C0). Therefore, in this investigation the study of the variation in shot volume is equivalent to analyze the effect of different SCF contents. Barzegari and Rodrigue[27] stated that an increase in the blowing agent content reduces the melt viscosity and, additionally, improves the number of nucleated cells. Thus, cells are created faster than the polymer solidification when it gets in contact with the cold mold wall. Consequently, as indicated in Figure 10, the skin thickness decreases and the cell density increases with the blowing agent content (reducing the shot volume). The gas is then distributed into a larger number of cells, reducing the probability of cell coalescence and decreasing their maximum size. The same effect of shot volume on cell density and size has been reported by Gómez-Gómez *et al.*[28] with Ethylene-Propylene-Block Copolymer (EPBC) foams. As the cells get smaller, the *CDI* parameter becomes closer to unity.

Concerning the mechanical properties, a higher level of shot volume involves a higher part weight and density, and obviously, a higher polymer fraction which can withstand the applied tensile load. As found by Li *et al.*[29] in microcellular Polyetherimide, the elastic modulus as well as the yield strength increase with the shot volume.

The effect of shot volume and gas content on the surface roughness is inconclusive (Figure 11). According to some experiments carried out by Peng *et al.*[30] with LDPE, PP and PS foamed through expandable thermoplastic microspheres, surface qualities decreased gradually with increasing content of blowing agent. Higher amounts of gas increase the surface roughness in bars injected at low mold temperature and injection velocity, but this

effect becomes unnoticeable as both the temperature in the cavity wall and the injection rate increase. Likewise, the influence of the mold temperature and injection velocity is greater at low shot volumes, suggesting the existence of an interaction effect between these three parameters.

Effect of mold temperature

The mold temperature has a much lower effect on the weight reduction than the shot volume. As it increases, the weight reduction ratio experiments a slight decrease, but it is closer to the proposed targets of 10% and 17%. Higher temperature in mold wall gives more time for foaming due to a longer cooling stage. Therefore a thinner solid surface layer is expected. In this study, a reduction in the skin thickness is observed in conditions where the molten polymer was injected at low velocity with 10% of weight reduction (C1 and C3). However, at higher injection rates, the observed trend is the opposite. This is also the case for the 17% of weight reduction. The combination of high injection rates and low shot sizes leads to high shear and gas content levels, which might counteract the effect of mold temperature on the thickness of the surface layer. An increase in skin thickness and cell density with the mold temperature is shown in Figure 10. The maximum cell diameter decreases at high levels of mold temperature in case of 10% of weight reduction, but increases in samples with 17% of weight reduction. Either way, the cell size distribution is constricted at higher temperatures in the mold wall, as indicated by the drop in the *CDI* parameter. The occurrence of an

interaction between processing parameters is clearly evidenced in this analysis, and it will be discussed further on in this work.

Bledzki *et al.*[17] obtained a decrease in the elastic modulus and tensile strength of PC foams as the mold temperature increased from 20 ºC to 108 ºC, due to the thinner solid skin, lower cell density and bigger cells formed. However, these trends are not observed in the injected ABS bars of this study, which may be due to the temperature range of the mold and its distance to the glass transition temperature T_g of the polymer. Verbeeten *et al.*[31] showed that mechanical properties, such as tensile strength, are influenced by the cooling profile of the material below T_g. The closer the mold temperature is to T_g, the effect of the mold temperature variations is more significant. In this work, the mold temperature ranges from 30 ºC to 60 ºC, while the T_g of ABS is around 100 ºC. Since the foaming process itself also influences cooling, the mold temperature variations appear not to be enough to significantly change the elastic modulus and tensile strength. As a matter of fact, the mold temperature does not appear in the regression models shown in Table 4 of any of the tensile properties studied in this work.

Mold temperature has been found as the most influencing parameter on the surface quality of ABS injection molded parts.[32] In this study, a clear effect of the mold temperature is observed but only at low levels of shot volume. The increase in mold temperature makes the melt flow easily, preventing the gas being trapped between the cavity wall and the melt polymer. Thus, smoother surfaces are obtained, as shown in Figure 11. Similar conclusions have been reported with other foamed materials, such as PP.[33]

Effect of injection velocity

The increase in the injection rate contributes to a lower ratio of weight reduction, but closer to the objectives of 10% and 17%. According to Figure 10, the solid skin is not affected by the injection rate in foamed bars with 10% of weight reduction. However, thinner surface layers are formed as the injection rate increases in case of 17% of weight reduction. Dong *et al.*[34] reported that when filling at high velocity, the effect of cooling is strongly reduced. The material keeps a relatively high temperature to allow the expansion of the foaming core, reducing the thickness of the surface layer. The injection velocity has been widely related to the pressure drop of the polymer/gas solution inside the mold cavity. As concluded by Mahmoodi and Behravesh[35], a high pressure drop improves cell nucleation, which turns into higher cell densities. However, it is quite noticeable the insignificant effect of the injection velocity on the cell density obtained in this research. The confinement of gas and polymer in a circular geometry could promote cell coalescence having a lower number of cells and then, the real influence of the injection rate on cell density cannot be determined. Gómez-Gómez *et al.*[36] reported that the effect of injection velocity on the cell density of PETG plates is inconclusive. Rizvi *et al.*[16] pointed out a decrease in cell diameter and *CDI* parameter with the injection velocity. In the present study, the maximum cell size decreases, however, the *CDI* increases drastically. That is, the cell size distribution becomes more heterogeneous, which might be due to the thick section of the cylindrical bars causing cell coalescence in the center of the specimens.

Lin *et al.*[14] reported an improvement of the tensile properties of ABS foams with the injection velocity, due to higher material orientation. In this study, the variation in elastic modulus and tensile strength obtained at the different injection rates are within the experimental accuracy, so the effect of the injection rate on the yield stress can be neglected.

Concerning the surface quality, both Average roughness (S_a) and Root mean square (S_q) decrease with increasing the injection velocity, being this effect greater at low levels of shot volume. Bociaga and Palutkiewicz[37] also found an improvement in surface gloss of HDPE molded foams at high injection rate. The faster injection causes a significant orientation of the polymer and an increase in melt temperature, easing filling of the cavity without surface defects. From Figure 11 it can be observed that as the injection velocity and mold temperature increase, S_a and S_q parameters of foamed series with 17% of weight reduction reach values in the same order as the ones of the 10% foamed bars. Hence, the negative effect of increasing the gas content on surface roughness can be counteracted by raising mold temperature and injection velocity. An interaction effect between these three analyzed factors is manifested.

Interaction between processing parameters

The presence of significant interaction effects between processing parameters can be concluded from the discussion above. An interaction effect between parameters occurred when the influence of one factor depends on the value of the other ones. The Pareto charts illustrated in Figure 12 point out the magnitude of the standardized effects (effects divided by their respective standard errors) caused by the different factors. The dashed line drawn

on the graphs indicates the minimum magnitude of statistically significance, with a confidence level of 95% (α = 0.05). Thus, the effects extending this reference line are potentially important. It is very clear from Figure 12(a) that the interaction between mold temperature and injection velocity has the highest effect on the solid skin thickness variability and sensitivity. Another response affected by an interaction between factors is the maximum cell size (Figure 12(b)). It is mainly influenced by shot volume, followed by the combination of mold temperature and injection velocity, whose effect on cell diameter is occasionally different depending on the level of each one. From the discussion above it has been also noticed an interaction effect between the shot volume, mold temperature and injection velocity on the surface roughness parameters (S_a and S_q) of the foamed bars.

CONCLUSIONS

In this study, solid and foamed cylindrical bars made of ABS were injection molded. The solid skin/foamed core structure of the cellular samples was analyzed, and their mechanical properties as well as surface quality were tested. A design of experiments was conducted in order to assess the effect of shot volume, mold temperature and injection velocity on the morphology, tensile properties and surface roughness. The following conclusions can be drawn from this study:

- The most influencing parameter on cell structure and mechanical properties is the shot volume and, indirectly, the SCF content. As the shot size decreased and the gas content increased, finer and more uniform cell structures were created, with higher cell densities and

narrower cell size ranges. However, enhanced elastic modulus and yield strength were obtained by increasing the shot size.

- The effect of the mold temperature and injection velocity is secondary. They are related to the cooling rate and pressure drop induced inside the mold cavity and, in general terms, higher levels of both parameters contributed to improve the morphology of the foamed parts for 10% and 17% weight reduction ratios (60 ºC and 100 cm^3 s^{-1}).

- The differences in mechanical properties obtained by varying mold temperature and injection rate lie within the experimental accuracy, so their effect on tensile strength and elastic modulus is negligible. The different foam morphologies obtained in this study do not seem to have a determinant influence on the tensile properties, which are mainly dependent on the apparent density.

- Interactions between processing parameters were found and in some cases had a greater effect than each factor independently. The statistical analysis of the factorial design of experiments demonstrated that the influence of the mold temperature on the solid skin thickness and cell size is different at different levels of injection velocity.

- Regarding the influence on the surface roughness, a strong dependence between the different factors was determined. For low mold temperature and injection velocity, the decrease in shot volume and increase in gas content led to poor surface quality. However, it could be greatly improved by raising both mold temperature and injection velocity.

- The optimal processing parameters depend on the material, thickness and geometry of the part. This investigation contributes to a better understanding about the general trends of the foaming behavior of ABS polymer at different injection molding conditions.

REFERENCES

1.   M.-Y. Lyu, T. Choi, *Int J Precis Eng Manuf* **2015**, 16, 213.

2.   D. Elduque, I. Claveria, A. Fernandez, C. Javierre, C. Pina, J. Santolaria, *Adv Mech Eng* **2014**, 2014, 1.

3.   H. C. Kim, T. J. Wallington, *Environ Sci Technol* **2013**, 47, 6089.

4.   H.-Y. Mi, X. Jing, M. R. Salick, W. C. Crone, X.-F. Peng, L.-S. Turng, *Adv Polym Tech* **2014**, 33, 21380.

5.   J. Gómez-Monterde, M. Sánchez-Soto, M. L. Maspoch, *Compos Part A Appl Sci Manuf* **2018**, 104, 1.

6.   J. Xu, *Microcellular injection molding*, Wiley, Hoboken, New Jersey **2010**.

7.   X. Sun, L.-S. Turng, E. Dougherty, P. Gorton, *Adv Polym Tech* **2012**, 31, 7.

8.   Y. Wang, G. H. Hu, *Appl Mech Mater* **2011**, 66, 2010.

9.   S.-C. Chen, Y.-W. Lin, R.-D. Chien, H.-M. Li, *Adv Polym Tech* **2008**, 27, 224.

10.   R. E. Murray, J. E. Weller, V. Kumar, *Cell Polym* **2000**, 19, 413.

11.   K. Nadella, V. Kumar, W. Li, *Cell Polym* **2005**, 24, 71.

12. G.-G. Lin, D.-J. Lin, L.-J. Wang, T.-W. Kuo, *Res Chem Intermed* **2014**, 40, 2259.

13. G. W. Dong, G. Q. Zhao, Y. J. Guan, G. L. Wang, X. X. Wang, *J Appl Polym Sci* **2014**, 131, 40365.

14. C.-K. Lin, S.-H. Chen, H.-Y. Liou, C.-C. Tian, presented at Society of Plastics Engineers Annual Technical Conference ANTEC, Boston, Massachusetts (USA), 2005.

15. L. Sorrentino, E. Di Maio, S. Iannace, *J Appl Polym Sci* **2010**, 116, 27.

16. S. Rizvi, M. Alaei, A. Yadav, N. Bhatnagar, *J Cell Plast* **2014**, 50, 199.

17. A. K. Bledzki, H. Kirschling, M. Rohleder, A. Chate, *J Cell Plast* **2012**, 48, 301.

18. A. Tsuchiya, H. Tateyama, T. Kikuchi, T. Takahashi, K. Koyama, *Polym J* **2007**, 39, 514.

19. Y. D. Hwang, S. W. Cha, *Polym Test* **2002**, 21, 269.

20. J. Gómez-Monterde, M. Schulte, S. Ilijevic, J. Hain, M. Sánchez-Soto, O. O. Santana, M. L. Maspoch, *J Appl Polym Sci* **2016**, 133, 43010.

21. K. K. Beydokhti, A. H. Behravesh, T. Azdast, *Iran Polym J* **2006**, 15, 555.

22. Z.-N. Yin, T.-J. Wang, *Appl Math Mech -Engl Ed* **2012**, 33, 455.

23. S. W. Cha, J. D. Yoon, *Polym-Plast Technol* **2005**, 44, 795.

24. D. C. Montgomery, *Design and analysis of experiments*, John Wiley & Sons, Hoboken, New Jersey **2008**.

25. C. M. Judd, G. H. McClelland, C. S. Ryan, *Data analysis: A model comparison approach*, Routledge, Abingdon, Oxon **2011**.

26. R. L. Mason, R. F. Gunst, J. L. Hess, *Statistical design and analysis of experiments: with applications to engineering and science*, Vol. 474, John Wiley & Sons, Hoboken, New Jersey **2003**.

27. M. R. Barzegari, D. Rodrigue, *Polym Eng Sci* **2009**, 49, 949.

28. J. F. Gómez-Gómez, D. Arencón, M. A. Sánchez-Soto, A. B. Martínez, *Adv Polym Tech* **2013**, 32, E692.

29. J. L. Li, Z. L. Chen, X. Z. Wang, T. Liu, Y. F. Zhou, S. K. Luo, *J Appl Polym Sci* **2013**, 130, 4171.

30. J. Peng, E. Yu, X. Sun, L. S. Turng, X. F. Peng, *Int Polym Proc* **2011**, 26, 249.

31. W. M. H. Verbeeten, M. J. W. Kanters, T. A. P. Engels, L. E. Govaert, *Polym Int* **2015**, 64, 1527.

32. M. J. Oliveira, A. M. Brito, M. C. Costa, M. F. Costa, *Polym Eng Sci* **2006**, 46, 1394.

33. S.-S. Hwang, J.-P. Yang, C.-H. Hu, P. Hsu, presented at Society of Plastics Engineers Annual Technical Conference ANTEC, Orlando (USA), 2015.

34. G. Dong, G. Zhao, Y. Guan, S. Li, X. Wang, *J Cell Plast* **2015**

35. M. Mahmoodi, A. H. Behravesh, *Iran Polym J* **2007**, 16, 839.

36. F. J. Gómez-Gómez, D. Arencón, M. A. Sánchez-Soto, A. B. Martínez, *J Cell Plast* **2013**, 49, 47.

37. E. Bociaga, P. Palutkiewicz, *Polym Eng Sci* **2013**, 53, 780.

FIGURE CAPTIONS
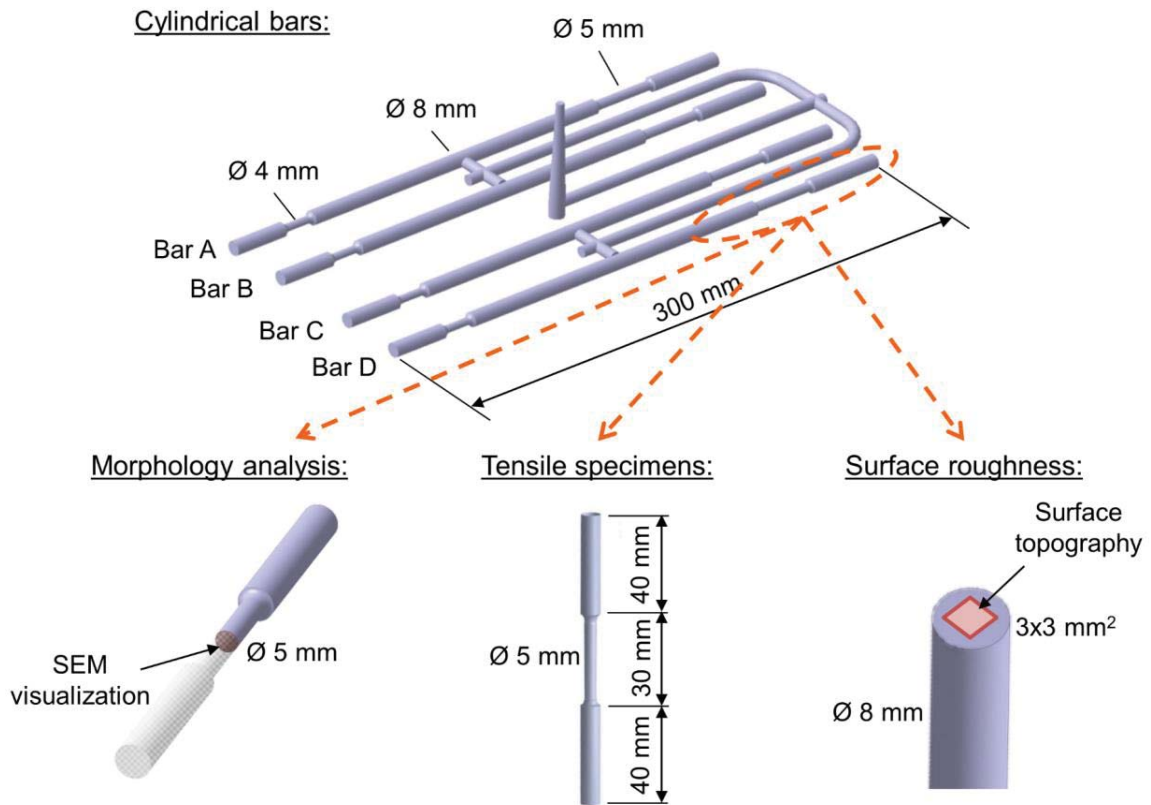
Figure 1. Scheme of sections for morphology and surface analysis and tensile test specimens extracted from the injected cylindrical bars.
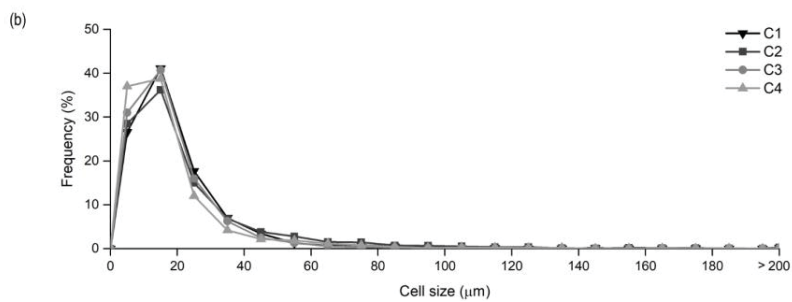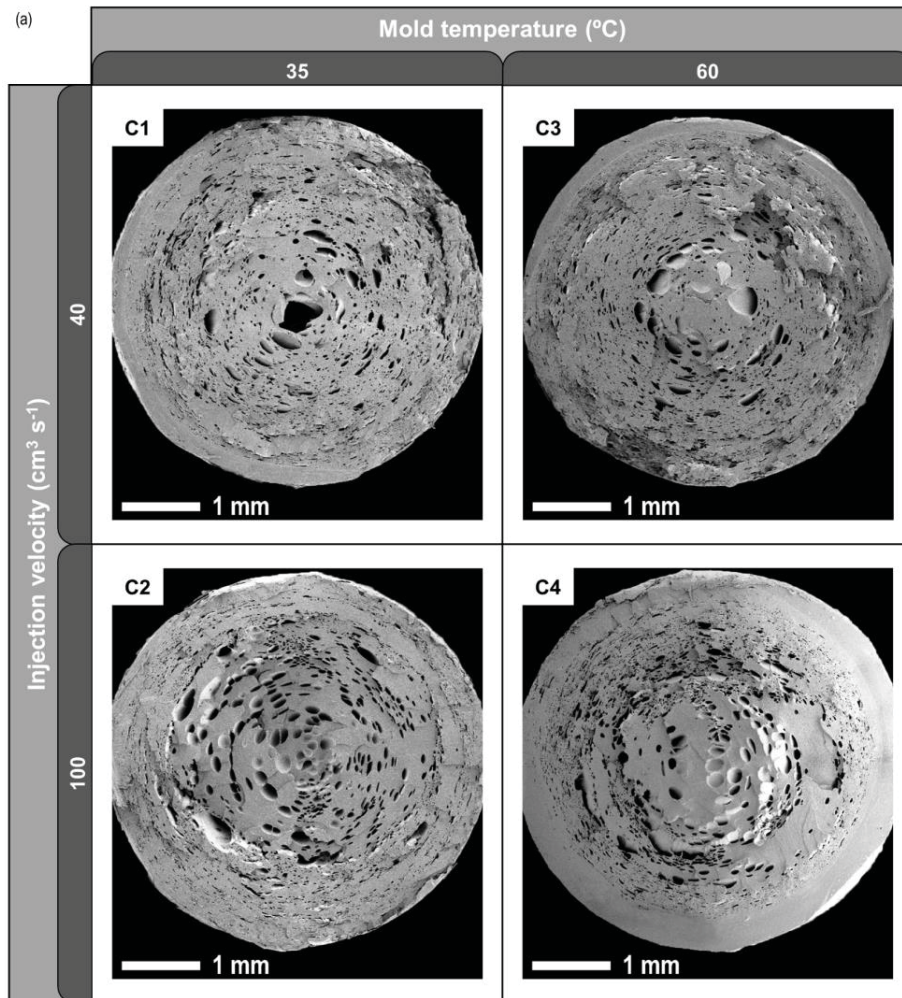
Figure 2. (a) SEM micrographs of C1-C4 conditions; (b) cell size distribution of C1-C4 conditions. Shot volume: 71 cm^3 (10% weight reduction).
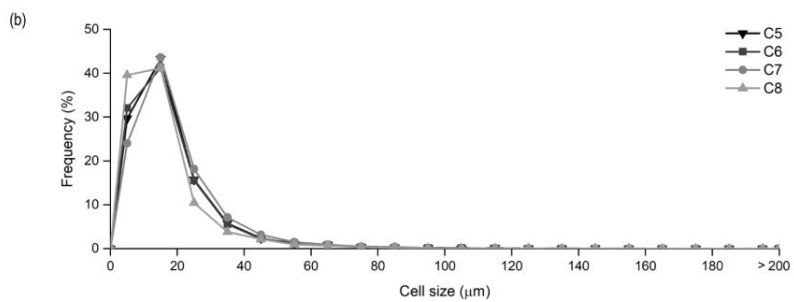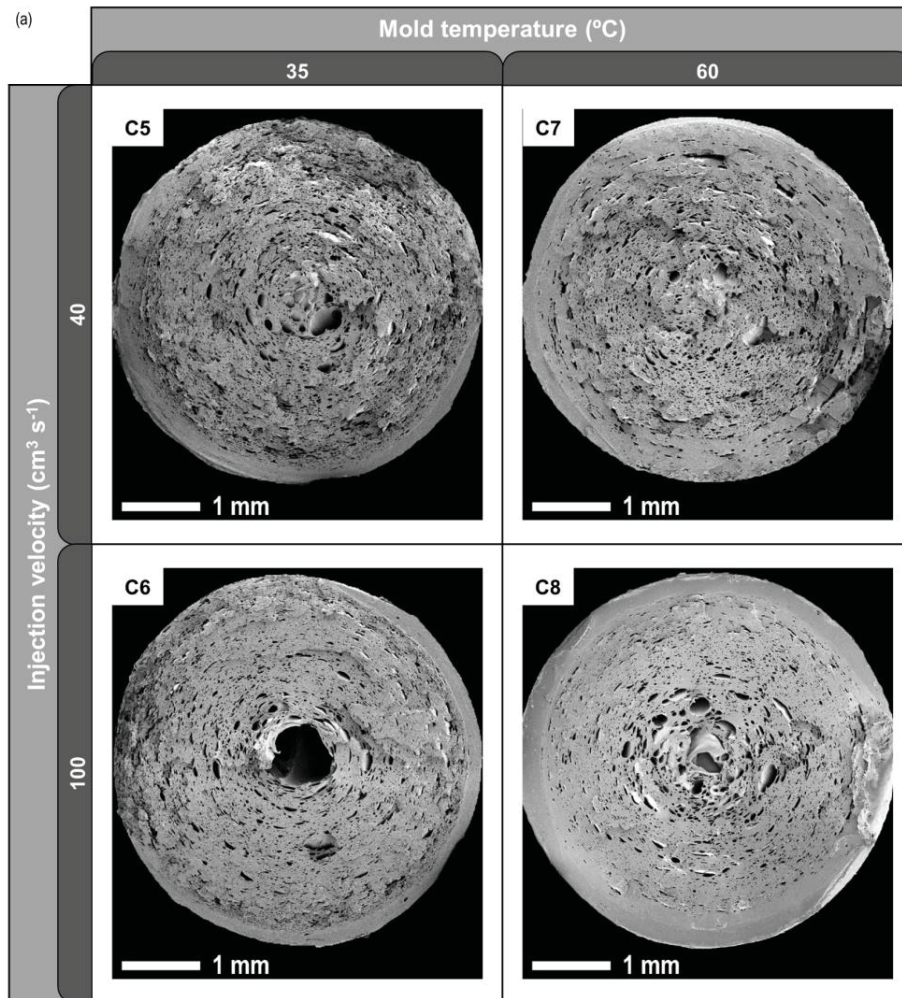
Figure 3. (a) SEM micrographs of C5-C8 conditions; (b) cell size distribution of C5-C8 conditions. Shot volume: 68 cm^3 (17% weight reduction).
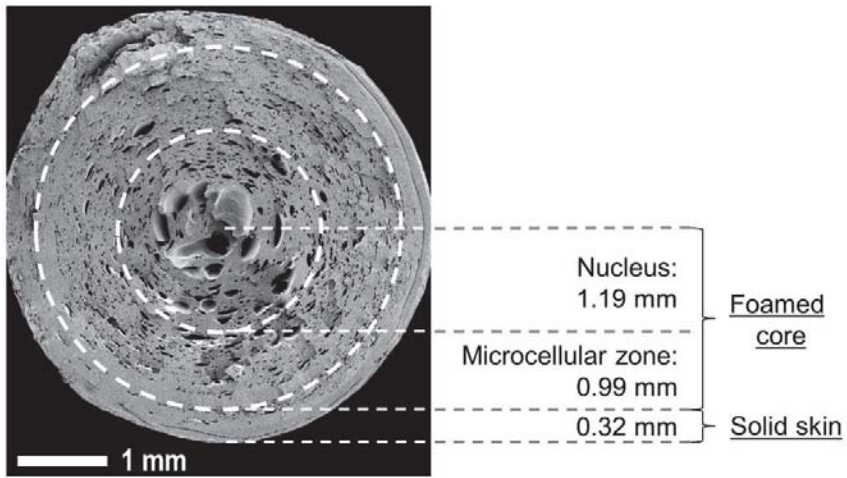
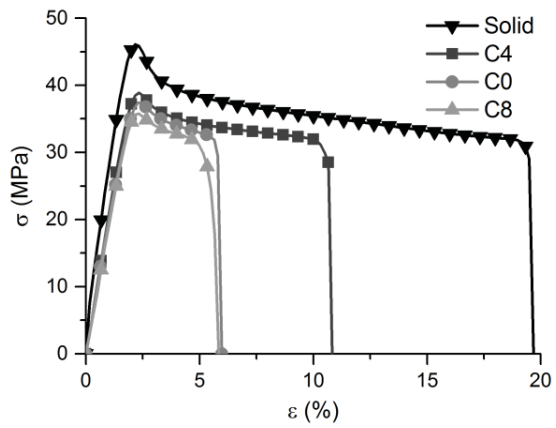**Figure 4.** SEM micrograph and morphology areas of C0 condition.

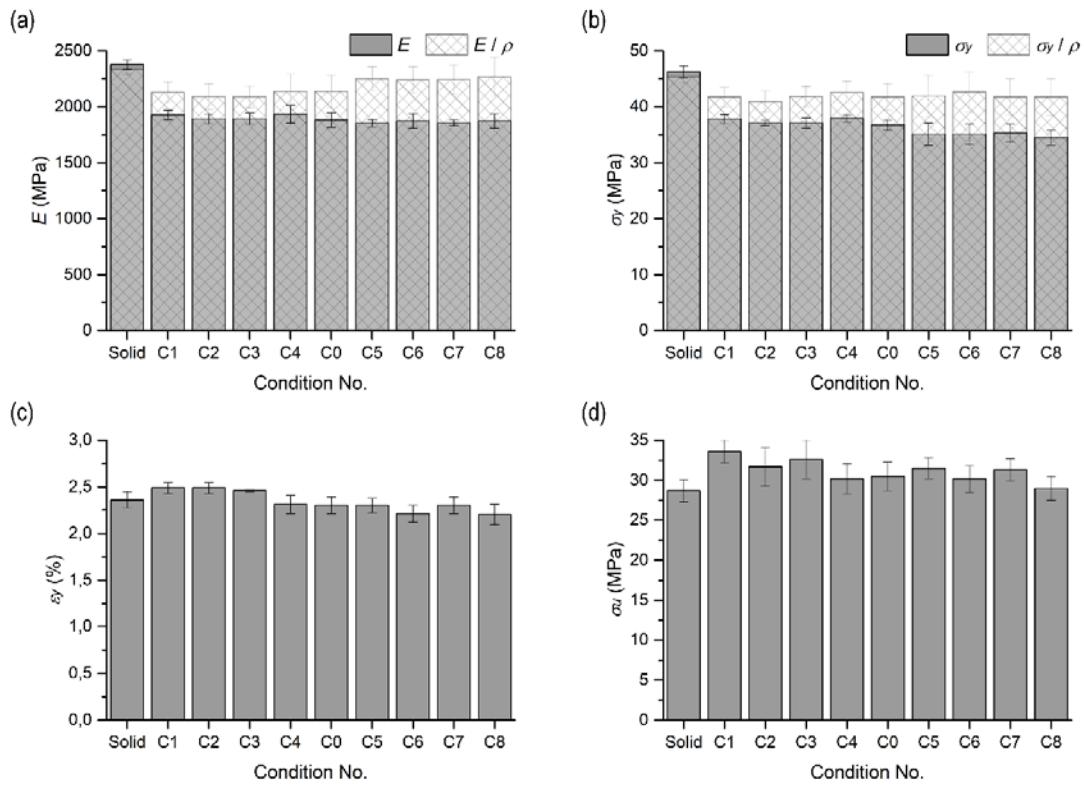**Figure 5.** Tensile stress-strain curves of solid and foamed samples (C4, C0 and C8 conditions).

Figure 6. (a) Elastic modulus (E); (b) yield strength (σ_y); (c) yield strain (ε_y); (d) ultimate strength (σ_u) of solid and foamed samples.
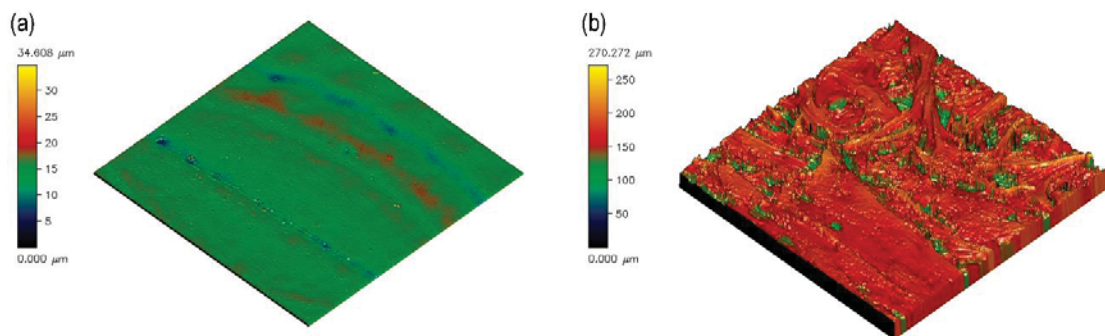

Figure 7. Surface topographies of injected bars at (a) solid; (b) foamed (C5) conditions.
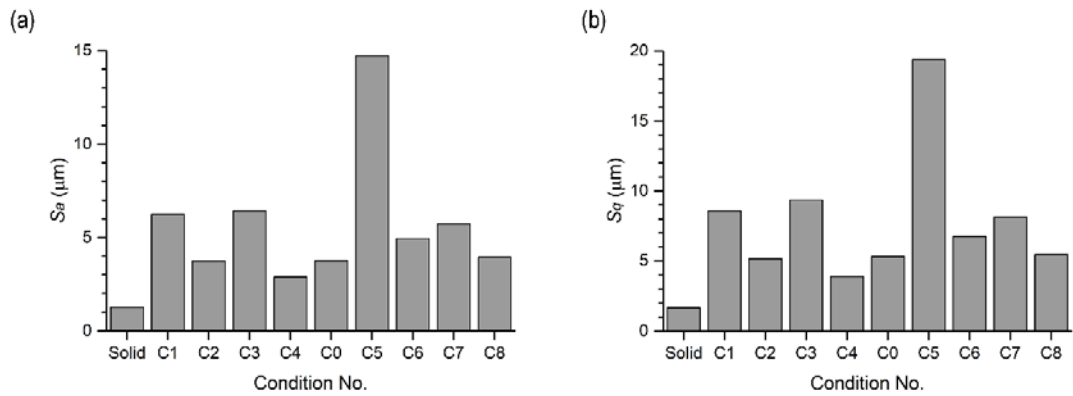
Figure 8. (a) Average roughness (S_a); (b) root mean square (S_q) of solid and foamed samples.
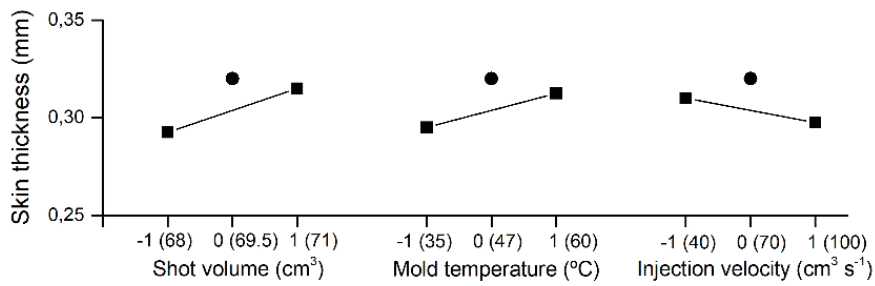

Figure 9. Main effect of shot volume, mold temperature and injection velocity on skin thickness.
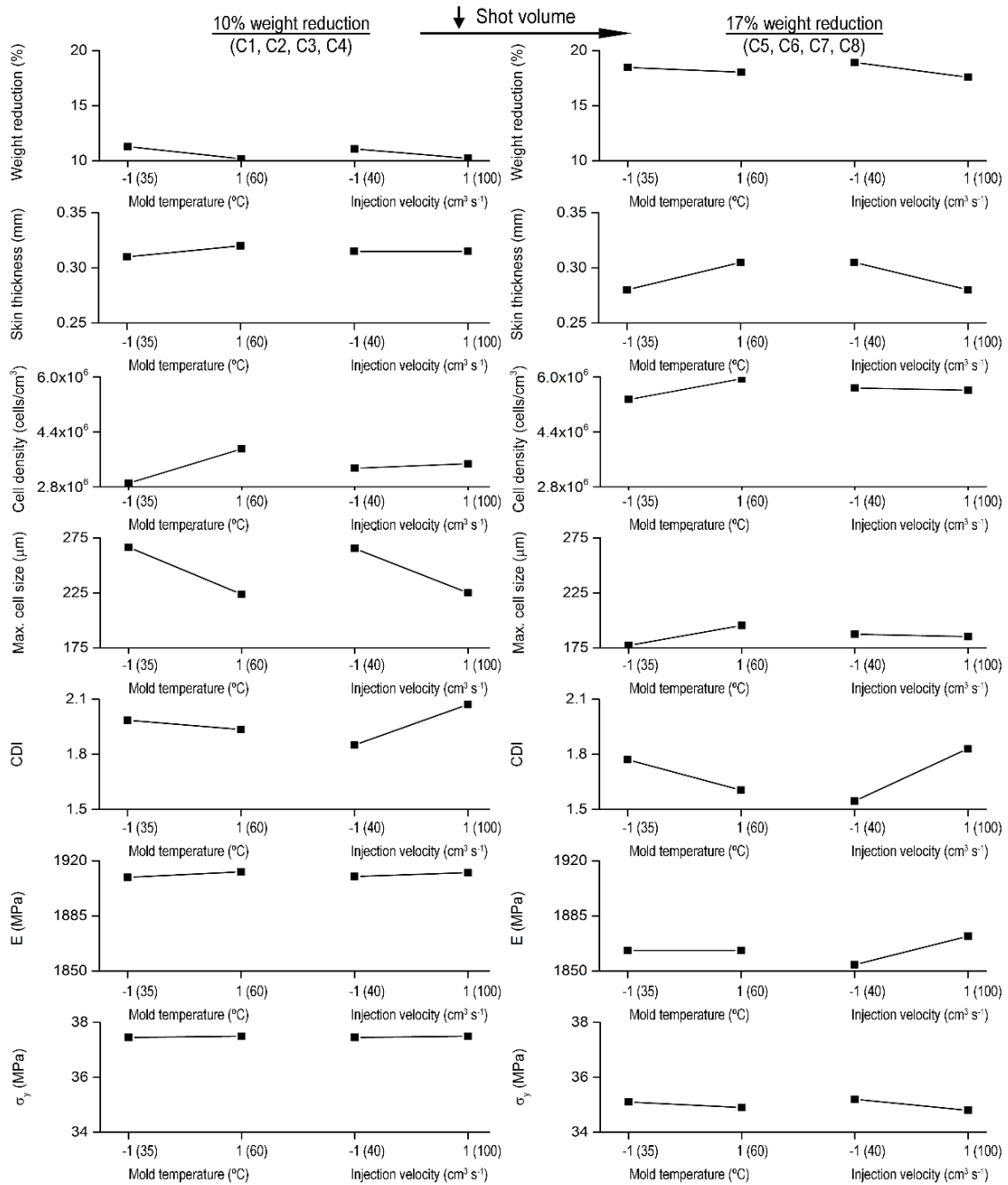
Figure 10. Effect of processing parameters on morphology and tensile properties of foamed bars.
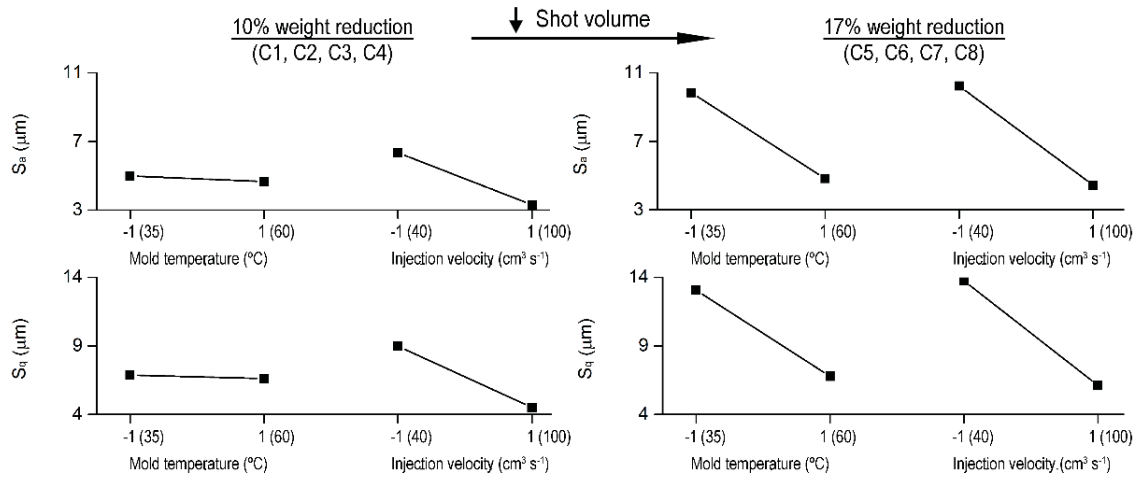
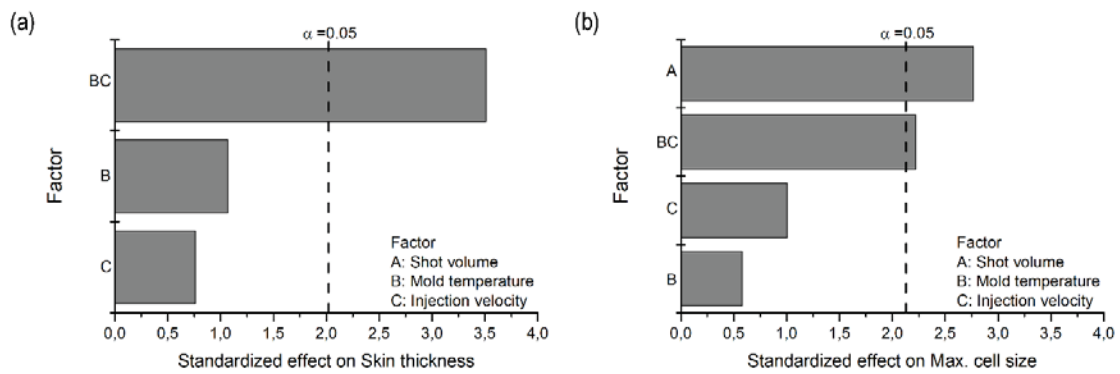**Figure 11.** Effect of processing parameters on surface roughness parameters of foamed bars.

Figure 12. Pareto charts of the standardized effect of processing parameters on (a) skin thickness; (b) maximum cell size.

Table 1. Factors and experimental domain for ABS microcellular injection molding. Note that values of 0 level are only employed in intermediate condition C0 (see Table 2) for linearity checking.

Factor	Levels		
	-1	0	1
Shot volume (cm^3)	68	69.5	71
Mold temperature (ºC)	35	47	60
Injection velocity (cm^3 s^{-1})	40	70	100

Table 2. Matrix of the Design of Experiments for ABS microcellular injection molding.

Condition No.	Shot volume	Mold temperature	Injection velocity
C1	1 (71 cm^3)	-1 (35 ºC)	-1 (40 cm^3 s^{-1})
C2	1 (71 cm^3)	-1 (35 ºC)	1 (100 cm^3 s^{-1})
C3	1 (71 cm^3)	1 (60 ºC)	-1 (40 cm^3 s^{-1})
C4	1 (71 cm^3)	1 (60 ºC)	1 (100 cm^3 s^{-1})
C5	-1 (68 cm^3)	-1 (35 ºC)	-1 (40 cm^3 s^{-1})
C6	-1 (68 cm^3)	-1 (35 ºC)	1 (100 cm^3 s^{-1})
C7	-1 (68 cm^3)	1 (60 ºC)	-1 (40 cm^3 s^{-1})
C8	-1 (68 cm^3)	1 (60 ºC)	1 (100 cm^3 s^{-1})
C0	0 (69.5 cm^3)	0 (47 ºC)	0 (70 cm^3 s^{-1})

Table 3. Weight reduction ratio, apparent density and morphological parameters of foamed samples.

Cond. No.	Weight reduction (%)	Density (g cm^{-3})	Skin thickness (mm)	Cell density (cells cm^{-3})	Cell size range (µm)	CDI
C1	11.14 ± 0.51	0.91 ± 0.02	0.35	3.1·10^6	8 - 271	1.87
C2	11.12 ± 0.64	0.91 ± 0.03	0.27	2.7·10^6	8 - 262	2.10
C3	11.03 ± 0.59	0.91 ± 0.02	0.28	3.6·10^6	8 - 260	1.83
C4	9.33 ± 0.33	0.91 ± 0.03	0.36	4.2·10^6	8 - 188	2.04
C5	19.09 ± 0.77	0.83 ± 0.03	0.31	5.4·10^6	8 - 147	1.57
C6	17.84 ± 1.12	0.84 ± 0.04	0.25	5.2·10^6	8 - 208	1.97
C7	18.76 ± 0.70	0.83 ± 0.02	0.30	5.9·10^6	8 - 228	1.52
C8	17.32 ± 0.48	0.83 ± 0.03	0.31	6.0·10^6	8 - 163	1.69
C0	13.55 ± 0.76	0.88 ± 0.03	0.32	5.1·10^6	8 - 240	1.92

Table 4. Regression models derived from factorial design analysis.

Response	Regression model (A: Shot volume; B: Mold temperature; C: Injection <mark>velocity</mark>)
Weight reduction	Weight reduction (%) = 14.353 - 3.799 A - 0.551 C
Skin thickness	Skin thickness (mm) = 0.30556 + 0.00875 B - 0.00625 C + 0.02875 B*C
Cell density	Cell density (cells cm^{-3}) = 4590851 - 1122047 A + 401962 B
Max. cell size	Maximum cell size (µm) = 218.5 + 29.5 A - 6.2 B - 10.6 C - 23.7 B*C
CDI	CDI = 1.8344 + 0.1363 A + 0.1262 C
E	E (MPa) = 1886.44 + 24.13 A
σ_y	σ_y (MPa) = 36.289 + 1.238 A
S_a	S_a (µm) = 5.821 - 1.257 A - 1.332 B - 2.204 C + 1.168 A*B
S_q	S_q (µm) = 8.00 - 1.59 A - 1.63 B - 3.03 C + 1.51 A*B

Table 5. Analysis of variance for skin thickness.

Source of Variation	Degrees of Freedom	Sum of Squares	Mean Square	F-value	p-value
Model	3	0.007537	0.002513	4.68	0.065
Mold temperature	1	0.000613	0.000613	1.14	0.334
Injection velocity	1	0.000313	0.000313	0.58	0.480
Mold temperature*Injection velocity	1	0.006613	0.006613	12.32	0.017
Residual	5	00.2685	0.000537		
Curvature	1	0.000235	0.000235	0.38	0.569
Lack of Fit	4	0.002450	0.000612		
Total	8	0.010222			